ORIGINAL PAPER

Wave propagations in crossing-fault tunnels and their effects on the dynamic response characteristics of tunnel surrounding rock

Danqing Song[1,2] · Wanpeng Shi[1] · Mengxin Liu[4] · Xin He[5] · Runhu Lu[3] · Jianwei Zhang[3]

Abstract

Seismic dynamic stability is a critical problem in crossing-fault tunnels. A three-dimensional model with a crossing-fault tunnel and infinite boundaries is established based on the finite-element method. By combing the results in time and frequency domains, a time–frequency conjoint analysis method is proposed to systematically investigate the seismic response characteristics of the surrounding rock and tunnel structures in the crossing-fault tunnel. The propagation of waves in the crossing-fault tunnel and its seismic amplification effect are clarified in time domains. In frequency domain analysis, the analysis results of Fourier spectrum and modal analysis are integrated to reveal the correlation of the predominant frequency of seismic waves, the natural frequency, and the characteristics of dynamic response in the surrounding rock. The results show that, as the main wave propagation channel, the fault controls the wave propagation characteristics in the surrounding rock. In the crossing-fault section, the dynamic amplification effect of the surrounding rock is significant, and instability deformation is most likely to occur. Furthermore, the influences of tunnels on the dynamic response in the surrounding rock and crossing-fault are different. In the frequency domain, as a result of the first-order and higher-order natural frequency, the overall and local deformation caused have a combined effect on the surrounding rock. This work can be a reference for the assessment and prevention of damage in the tunnel under earthquake.

Introduction

The topographic and geological conditions in western China are extremely complicated (Lu and Cai 2019), which changes the construction of tunnels. (Song et al. 2020a, b).

✉ Mengxin Liu
liumengxin@nefu.edu.cn

1 School of Civil Engineering and Transportation, South China University of Technology, Guangzhou 510640, Guangdong, China

2 State Key Laboratory of Subtropical Building and Urban Science, South China University of Technology, Guangzhou 510640, Guangdong, China

3 School of Civil Engineering and Architecture, Henan University, Kaifeng 475004, China

4 School of Civil Engineering, Northeast Forestry University, Harbin 150040, China

5 China Construction Fifth Engineering Division Co., Ltd., Changsha 410000, China

Tunnel engineering is often faced with various disasters, such as rock bursts, gas outbursts, water outbursts, and mud outbursts, which have adverse effects on the construction, operation, and maintenance of tunnel engineering (Li et al. 2019). The stability of the surrounding rock in the crossing-fault section is an unavoidable engineering problem in tunnel construction, which seriously threatens the safety and operation of project construction (Fig. 1) (Yu et al. 2016). The coupling of the seismic load and complex geological conditions leads to strong dynamic responses in crossing-fault tunnels, which finally rise up to the generation and expansion of cracks and water inrush in the surrounding rock (Li and Ma 2009; Li et al. 2014). The mechanism of seismic damage in crossing-fault tunnels has to be revealed urgently in tunnel engineering.

The seismic response of the surrounding rock in crossing-fault is a scientific problem involving many domains (Song et al. 2021; Yan et al. 2020). Research on the dynamic response of crossing-fault tunnel surrounding rock based on the time domain and frequency domain is

Fig. 1 Earthquake damage in cross-fault tunnels (Yu et al. 2016)

beneficial for revealing the seismic response characteristics of surrounding rock from multiple perspectives (Fan et al. 2020; Shen et al. 2020; Song et al. 2020a, b). In the time domain, the seismic response characteristics of the rock surrounding a tunnel are investigated from the perspectives of mechanics and deformation, and their interaction mechanism is intuitively revealed (Cividini et al. 2010; Huang et al. 2017). At present, time domain analysis based on acceleration, velocity, displacement, and strain time history has become a common method to evaluate the seismic response of crossing-fault tunnels (Aygar and Gokceoglu 2021; Sun et al. 2020). Some scholars have explored the dynamic response law of crossing-fault tunnels surrounding rock under earthquakes based on time domain analysis (Geng et al. 2019; Li et al. 2019; Ma et al. 2019). The influence of seismic parameters and geological factors on the dynamic response characteristics of tunnels can be well explored by time domain analysis. However, due to the complex frequency components of seismic waves and the nonuniformity and anisotropy of rock−soil masses, some frequency components of waves have a great influence on the dynamic characteristics of the surrounding rock (Song et al. 2019). Therefore, it is difficult to fully reveal the influence mechanism of the frequency components of waves on the vibration characteristics of the surrounding rock in the time domain. Special attention should be given to further investigations in the frequency domain.

In the frequency domain, the seismic response of a complex tunnel surrounding rock mass is the result of the joint action of different frequency components of waves, surrounding rock, and tunnel structure (Shi et al. 2024; Song et al. 2024). Some scholars have studied the dynamic characteristics of tunnels based on the frequency domain. For example, (Liu et al. 2012; Pai and Wu 2021; Song et al. 2019; Wei et al. 2019) explored the dynamic response characteristics of surrounding rock by analysing the spectrum characteristics of the acceleration dynamic response of tunnels. The results show that frequency domain analysis can reveal the relationship between the remarkable frequency of waves, the natural frequency of tunnels, and their dynamic response characteristics (Geng et al. 2020; Sun et al. 2009). In addition, as an important part of the frequency-domain analysis, modal analysis can effectively reflect the relationship between the natural frequency of engineering entities and their deformation response characteristics (Dou et al. 2018). However, modal analysis has not been widely used in tunnel engineering. Hence, the frequency-domain research content can be further improved by incorporating modal analysis into the frequency-domain research of tunnel engineering. So, the spectrum characteristics, the mutual verification, and the supplement of modal analysis results can be fully considered. For crossing-fault tunnels, the complex geological structure leads to the complexity of dynamic characteristics. Therefore, it is particularly necessary to carry out frequency-domain research.

The study of the dynamic response of the surrounding rock in crossing-fault tunnels has great value in tunnel engineering (Long et al. 2023). At present, tunnel engineering construction is mainly in the highly seismic region of China. The complex geological structures of surrounding rocks in cross-fault sections make the construction and operation of tunnel engineering face the problem of complex geological conditions under earthquakes (Liang et al. 2021). The seismic load propagates in the form of waves across the fault surrounding rock, which causes the change of the original stress field and instability of the crossing-fault tunnel. Due to the complex interaction of faults, tunnels, and seismic waves, the seismic dynamic response and disaster mechanism of the rock surrounding a crossing fault become complex (Xu et al. 2021). In addition, many scholars have carried out relevant studies and made some progress on the dynamic response in tunnels surrounding rock under earthquakes (Liu et al. 2021; Xin et al. 2022). However, due to the

discontinuity of the surrounding rock and the complexity of waves, it is difficult to fully understand its seismic response characteristics and disaster mechanism. Most of the previous studies have studied the dynamic response characteristics of tunnels surrounding rock from the perspective of the time domain. However, it is difficult to fully reveal the dynamic response law of tunnels only from the analysis of the time domain. The present study also does not reveal the relationship between the seismic wave preeminent frequency, the natural frequency, and dynamic response characteristics of tunnel surrounding rock from the frequency domain. The modal analysis does not incorporate frequency-domain analysis in the research of tunnel dynamic response. The characteristics of dynamic response in the across-fault tunnel cannot revealed from the frequency domain. In addition, previous studies have not fully explored the propagation characteristics of seismic waves in intact surrounding rock, faults, and lining structures. The interaction mechanism between tunnels and surrounding rock is unclear. Therefore, this work has carried out in-depth and systematic research on the above problems.

In this work, taking a crossing-fault section of a tunnel in Fujian Province, China, as an example (Fig. 2), a three-dimensional finite element model with an infinite boundary is established. A time–frequency conjoint analysis method combining time and frequency domain analysis is proposed to study the dynamic response characteristics of the surrounding rock in a crossing-fault tunnel under an earthquake. The influence of the tunnel structure and fault on wave propagation characteristics is studied by analysing the transmission characteristics of waves in the surrounding rock mass. By analysing the characteristics of wave propagation, acceleration response, modal shape, and Fourier spectrum response, the dynamic response of crossing-fault surrounding rock is systematically investigated. The influence of faults and tunnels on the dynamic amplification effect of the surrounding rock is explored too. Combined with modal analysis and Fourier spectrum analysis, the correlation mechanism between the predominant frequency of a wave, the natural frequency of crossing-fault surrounding rock, and its deformation response characteristics is clarified. This work can provide a new method for revealing the disaster mechanism of surrounding rock under earthquakes and provide a scientific basis for seismic fortification of crossing-fault tunnels.

Numerical modelling

Case study

The tunnel is located in the tectonic erosion geomorphic area, and the site mainly passes through the hills and mountains, with an altitude of approximately 70–145 m (Fig. 3). In the field, the main component of the stratum structure is granite and the locally distributed interlayer with filling soil. According to the site geological survey, site borehole sampling, shear wave velocity test, and geophysical interpretation, the lithology of the slope is divided into strongly weathered granite, moderately weathered granite, and breezed granite, from top to bottom. The study area is mainly controlled and affected by two fault zones and a linear structure, which is characterized by dynamic metamorphism and extrusion fracture. Regional neotectonics movement is characterized by the differential movement of fault blocks. The fractures and fissures were mainly in the NNE direction, accompanied by diabase dike intrusion, and the movement gradually weakened after the late Pleistocene. The proposed tunnel area is mainly controlled by the SE fault. Two fault fracture zones (F5 and F6) were found in the area. Fault fracture zone F5 is approximately 20 m wide, occurrence NE22°/SE∠80° (Fig. 4). Fault fracture zone F6 is approximately 20–50 m wide, NE30°/SE∠77°. The joint inclination angles of F5 and F6 are 30–60° with the axis of the hole. Most of the fault zones are closed and have poor water conductivity and hydrophilicity, which have little effect on tunnel construction. In the proposed tunnel site, the surface water system and the water body are not developed, and no surface water distribution was observed during the investigation. Many earthquakes have historically occurred near the study area, and the geological disasters caused by earthquakes deserve our attention. To ensure the safe construction and operation of tunnels, it is very important to study the dynamic stability of crossing-fault tunnels. The tunnel surrounding rock—lining structure system at the interface between F5 and tunnel is selected as the research object. The surrounding rock of the tunnel is breezed granite. The tunnel surrounding rock and fault section were sampled and processed into cylindrical rock samples. A series of rock mechanics tests were carried out to obtain the physical and mechanical parameters of surrounding rock and fault. These tests mainly include rock static and dynamic triaxial test, Brazil splitting test, ultrasonic test, uniaxial compressive test, etc. They are used to obtain Poisson's ratio, elastic modulus, internal friction angle and cohesive force of surrounding rock and fault. The physical and mechanical constants of the surrounding rock are shown in Table 1.

Numerical modelling

The propagation of seismic waves in a rock mass can be modelled by assuming that the rock mass medium is continuous or discontinuous. In finite element dynamic analysis, optimizing the boundary conditions, degree, and subdivision size of the finite element model is of great significance to accurately simulate the wave propagation

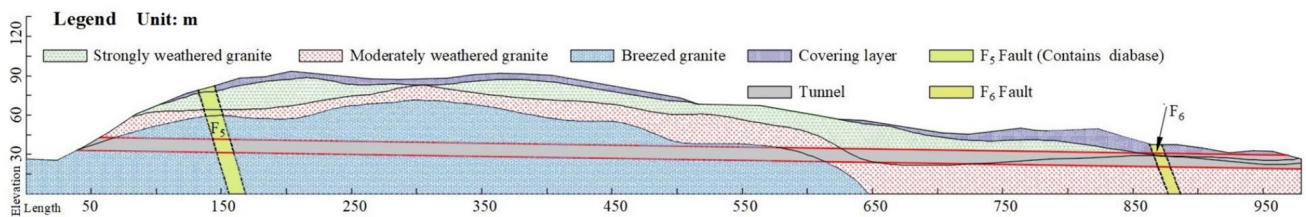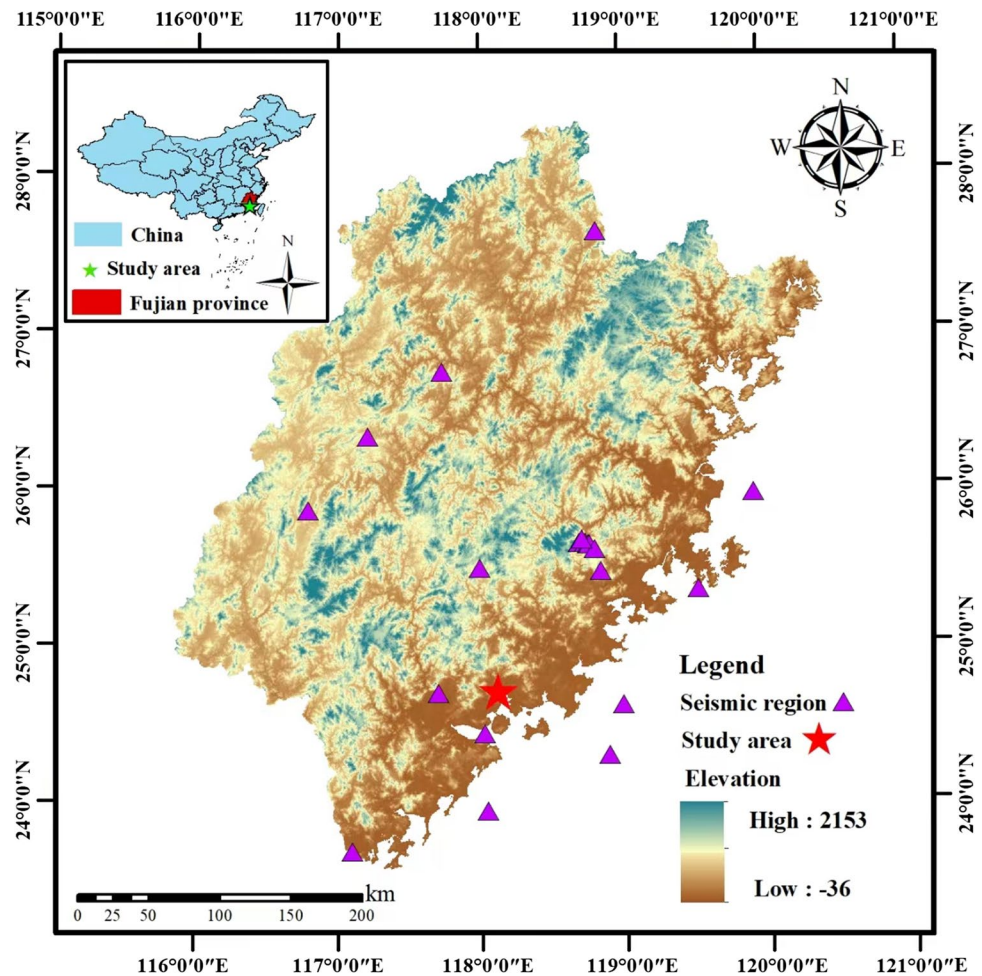**Fig. 2** Location of the study area

Fig. 3 Geological section of the tunnel engineering

(Song et al. 2021). In the continuum model, discontinuity construction such as faults, joints, and cracks is treated as special joint elements. To simulate rock mass fractures, Ngo and Scordelis (1967) proposed a two-node joint element to represent rock mass joints. Goodman and Bray (1976) proposed the joint element and developed the finite element method. The Goodman joint element is a linear element suitable for two-dimensional analysis. It has four joints without thickness. The stiffness matrix of the joint element is derived by the same method as the conventional finite element method. Mehtab and Goodman extended

the Goodman node element to three-dimensional finite element calculation (Mahtab 1970). Calculation accuracy and efficiency should be considered when grid division is carried out. Kuhlemeyer and Lysmer (1973) believe that the size of grid cells should not be 1/8–1/10 of the shortest wavelength, and grid encryption should be carried out in key research areas. When the elastic wave passes through the surface of the structure, part of the energy is transmitted, and part of the energy is refracted, reflected, and converted (Kumar and Kaur 2014). Obviously, the amplitudes of transmitted and reflected waves are closely
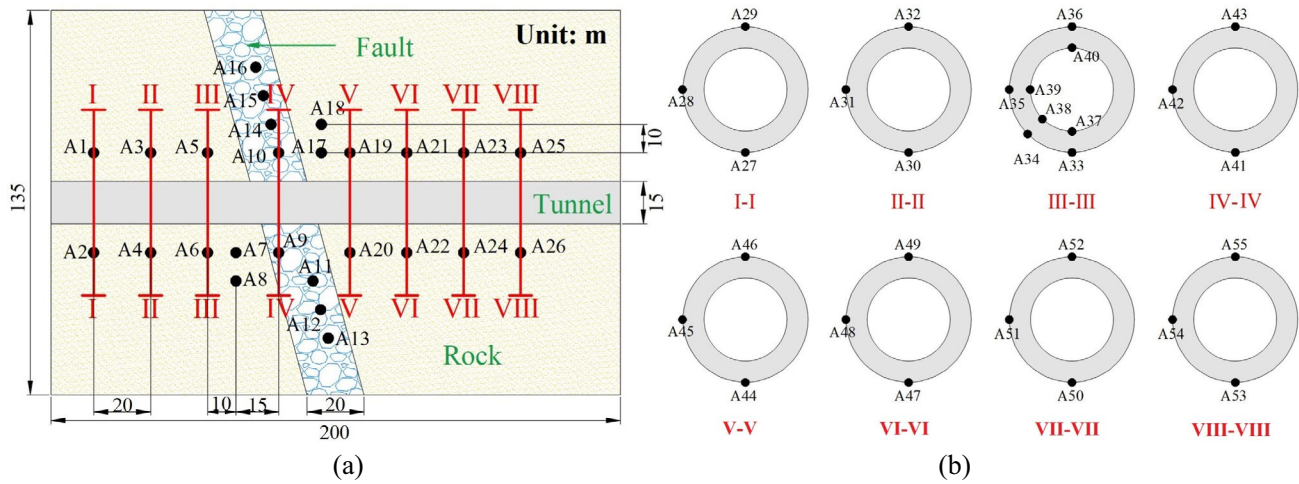
Fig. 4 Layout diagram of measuring points of the numerical model: **a** surrounding rock; **b** lining structure of the cross-fault tunnel

Table 1 Physical and mechanical constants of the tunnel surrounding rock—lining structure system

Lithology	Volumetric weight ρ/ kN/m³	Poisson's ratio μ	Elastic Modulus E/ GPa	Shear Modulus G/ GPa	Internal friction angle φ/°	Cohesive force c/ kPa
Surrounding rock	27	0.23	25	10.16	55	1800
Fault fracture zone	16	0.4	0.5	0.18	10	50
Lining structure	24	0.2	30	12.5	/	/

related to their frequency content, weak structural plane, length, spacing, thickness, and other geometric characteristics (Kumar and Kaur 2014). In this model, the surrounding rock is set as a quadrilateral grid, and the lining is set as a single-layer grid. In the process of dynamic analysis, the influence of different physical properties of the fault and surrounding rock on wave propagation characteristics is mainly considered. By using the "tie connection" method, the connection between the fault and the complete surrounding rock is set as "nonsurface contact" without setting viscous damping. The fault is modelled as a material softer than the surrounding rock, with a range size larger than the wavelength and a thickness value less than the wavelength. When the reflection coefficient of the interface between the fault and surrounding rock is large, multiple wave reflections should be considered. The main effect of faults on incident wave propagation is the deceleration and attenuation of incident waves.

The setting of the boundary conditions is the key factor affecting the dynamic analysis of the tunnel. The actual tunnel foundation is infinite, but the boundary size in the finite element model is finite. How to use the finite element model to simulate the actual infinite boundary and make the analysis result more reasonable is an important influencing factor in finite element dynamic analysis. In this model, the

infinite element boundary method is adopted to simulate the infinite foundation of the rock surrounding the tunnel, and the artificial truncation method is adopted to minimize the reflection and scattering of seismic waves on the model boundary (Bettess and Zienkiewicz 1977). The infinite element boundary is introduced into the finite element model. The infinite element boundary condition is applied on both the side of the slope and the bedrock of the model. The radiation energy of surface waves is absorbed by the infinite element boundary to reduce the adverse effects of reflected waves in dynamic analysis (Song et al. 2021). The seismic load is input into the bottom node of the model to simulate ground motion. The seismic wave propagation in the far-field region is simulated by infinite elements, and the seismic wave propagation in the near-field region is simulated by the finite element method. Infinite elements can directly absorb the reflection and scattering of seismic waves on the boundary, so the removal of high-frequency noise can be considered without affecting the effective periodic component of stress waves near the sliding surface. In the finite element dynamic calculation, in the case of an elastic medium, the stress generated by damping depends on the following formula (Madsen 1983):

$$\sigma_{xx} = -d_p \, \dot{\mu}_x \tag{1}$$

$$\sigma_{xy} = -d_s \, \dot{\mu}_y \tag{2}$$

$$\sigma_{xz} = -d_s \, \dot{\mu}_z \tag{3}$$

where $\dot{\mu}_x$, $\dot{\mu}_y$, and $\dot{\mu}_z$ represents the vibration speed. σ_{xx}, σ_{xy}, and σ_{xz} represent the stress generated by damping. The reflection energy of the P-wave and S-wave can be reduced by setting the coefficient. The energy reflection of longitudinal wave and shear wave can be slowed down by selecting the constants d_p and d_s.

In this model, the mesh of the surrounding rock is set as quadrilateral, and the mesh of the structural plane is set as single-layer. The size of the numerical model is 200 m (length) × 100 m (width) × 135 m (height). Based on the actual engineering situation, a circular tunnel lining structure with an inner diameter of 15 m and a lining thickness of 0.3 m is established. The fault fracture zone traversed was set as the normal fault, the angle between it and the horizontal direction was 60°, 75°, and 90°, and the width of the fault zone was 20 m. In the three numerical models, faults and linings are connected with adjacent surrounding rocks by tie constraints. To avoid the influence of element size on seismic wave transmission, the element size was set as 3 m, and the C3D8 element was used for grid mesh. In addition, the "seed edge" method is adopted to set the infinite unit for the numerical model on the outside. Finally, the total number of 60° model elements was 127029, including 107010 surrounding rock elements, 12915 fault elements, 1105 lining elements, and 5999 infinite element elements. The total number of 75° model elements is 126140, of which 106554 surrounding

rock elements, 12642 fault elements, 1056 lining elements, and 5888 infinite element elements. The total number of 90° model elements is 123480, of which there are 104,052 surrounding rock elements, 12,558 fault elements, 1040 lining elements, and 5,830 infinite element elements.

Because only the dynamic response characteristics of the tunnel under small deformation conditions are studied, the model material is regarded as elastic in finite element dynamic analysis. The dynamic response characteristics of the rock mass and lining structure in the online elastic domain are considered, and the Mohr–Coulomb criterion is used for the rock mass and lining structure materials. To avoid the influence of gravity on the tunnel rock mass, the stress balance calculation should be carried out before the dynamic calculation. The physical and mechanical parameters of the model are shown in Table 1. The numerical model of the crossing-fault tunnel is shown in Fig. 5. The artificial synthetic wave (AS wave) simulations are based on past earthquakes and geological structures in the area. The acceleration time history of the AS wave and its Fourier spectrum are shown in Fig. 6. At the bottom boundary of the model, an AS wave (0.01 g) was used for loading. The preeminent frequency of the AS wave is 2.5–3.5 Hz, and the input holding time is t = 40 s, Δt = 0.005 s.

Dynamic response characteristics in the time–frequency

Wave propagation characteristics

To explore the influence of faults and other discontinuities on seismic wave propagation characteristics, a certain acceleration propagation process in the surrounding rock underground motion is selected for analysis, as shown in Fig. 7.
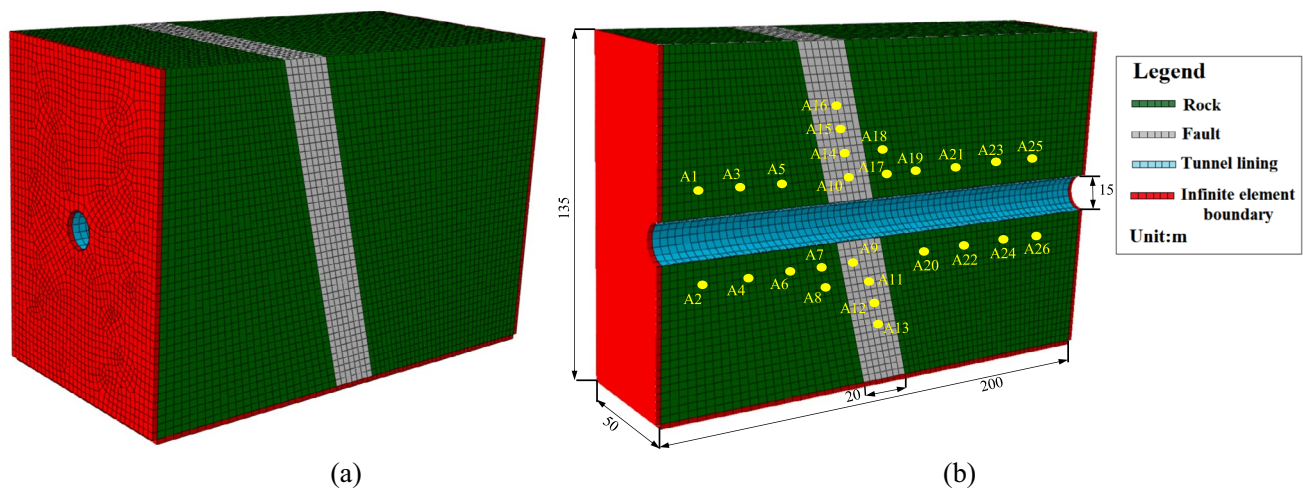

(a)   (b)

Fig. 5 Mesh model of the cross-fault tunnel (unit: m): **a** FEM model; **b** profile of the model

Fig. 6 Input seismic wave: **a** acceleration time history; **b** Fourier spectrum
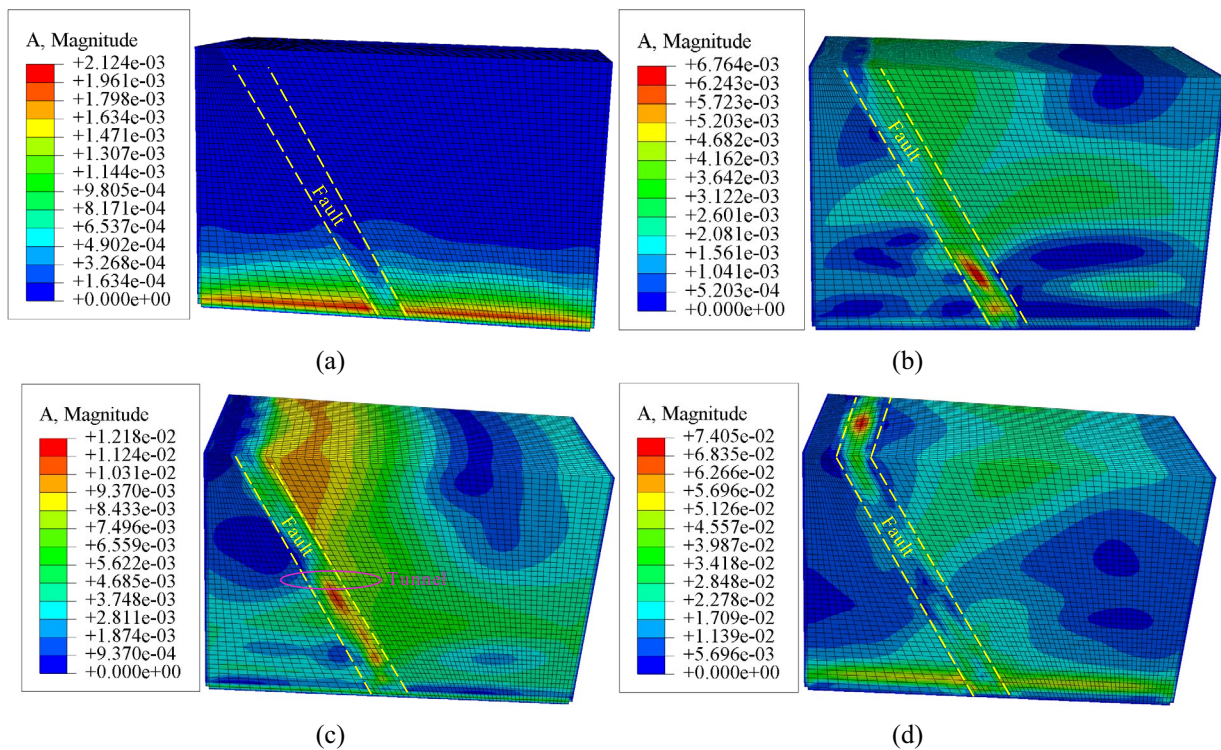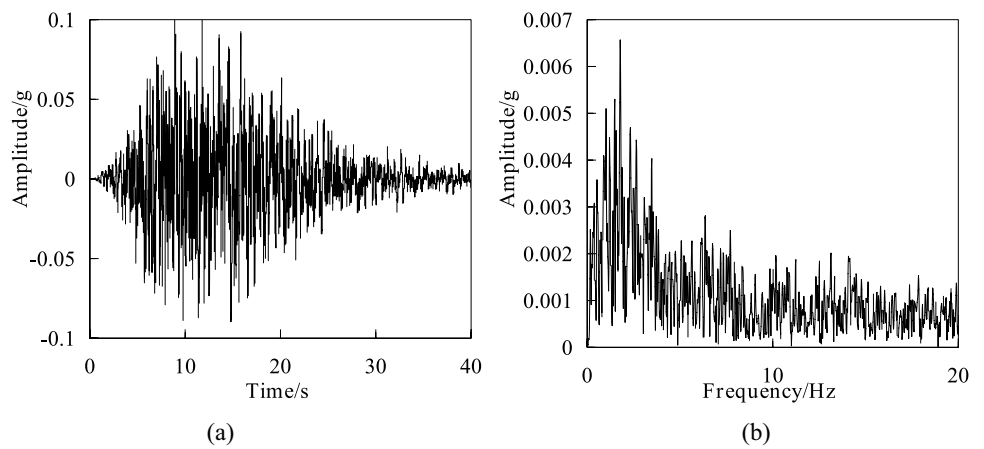

(a)

(b)

(a)

(b)

(c)

(d)

Fig. 7 Characteristics of seismic wave propagation in rock mass: **a** t = 0.02 s; **b** t = 0.05 s; **c** t = 0.72 s; **d** t = 1.36 s (Unit: m/s.²)

When the acceleration propagates across the surrounding rock area of the fault tunnel, it first exhibits layered propagation characteristics in the intact surrounding rock. With increasing elevation, the maximum acceleration gradually appears in the fault area. In other words, the seismic wave mainly concentrates its energy in the fault section and transmits gradually along the fault area. Meanwhile, from Fig. 7a to Fig. 7d, the peak ground acceleration (PGA) gradually shows an increasing trend. This indicates that the fault has a controlling effect on the wave propagation characteristics in the tunnel surrounding the rock. In the process of wave propagation, the fault is the main transmission channel of ground

motion energy and has the effect of amplifying the transmission process of waves. Wave propagation in the homogeneous rock medium is an attenuation phenomenon. However, the rock mass in the fault area and the intact surrounding rock belong to different media for the propagation of waves. When the wave propagates in the fault area, there are many refraction and reflection phenomena of seismic waves on the contact surface between the fault and intact surrounding rock, resulting in the superposition effect of the wave field in the fault. This causes the concentration of seismic wave energy in the fault area, which leads to the amplification effect on the wave field in the fault area as well.

In addition, to study the seismic wave propagation characteristics of the tunnel lining structure underground motion, the lining structure in the model in Fig. 7 is separately extracted, as shown in Fig. 8. The PGA of the lining structure is mainly concentrated in the crossing-fault segment during earthquakes. The dynamic amplification effect of the tunnel lining structure across fault segments is the largest. The fault changes the distribution characteristics

of the acceleration of the tunnel structure, and the ground motion energy is concentrated in the tunnel structure across the fault. In addition, Fig. 9a shows that the PGA of the surrounding rock in the fault increases with the relative elevation during wave propagation, especially in the area above the tunnel, and the PGA of the surrounding rock in the fault shows a sudden increase. This shows that the dynamic amplification effect of the tunnel structure on the
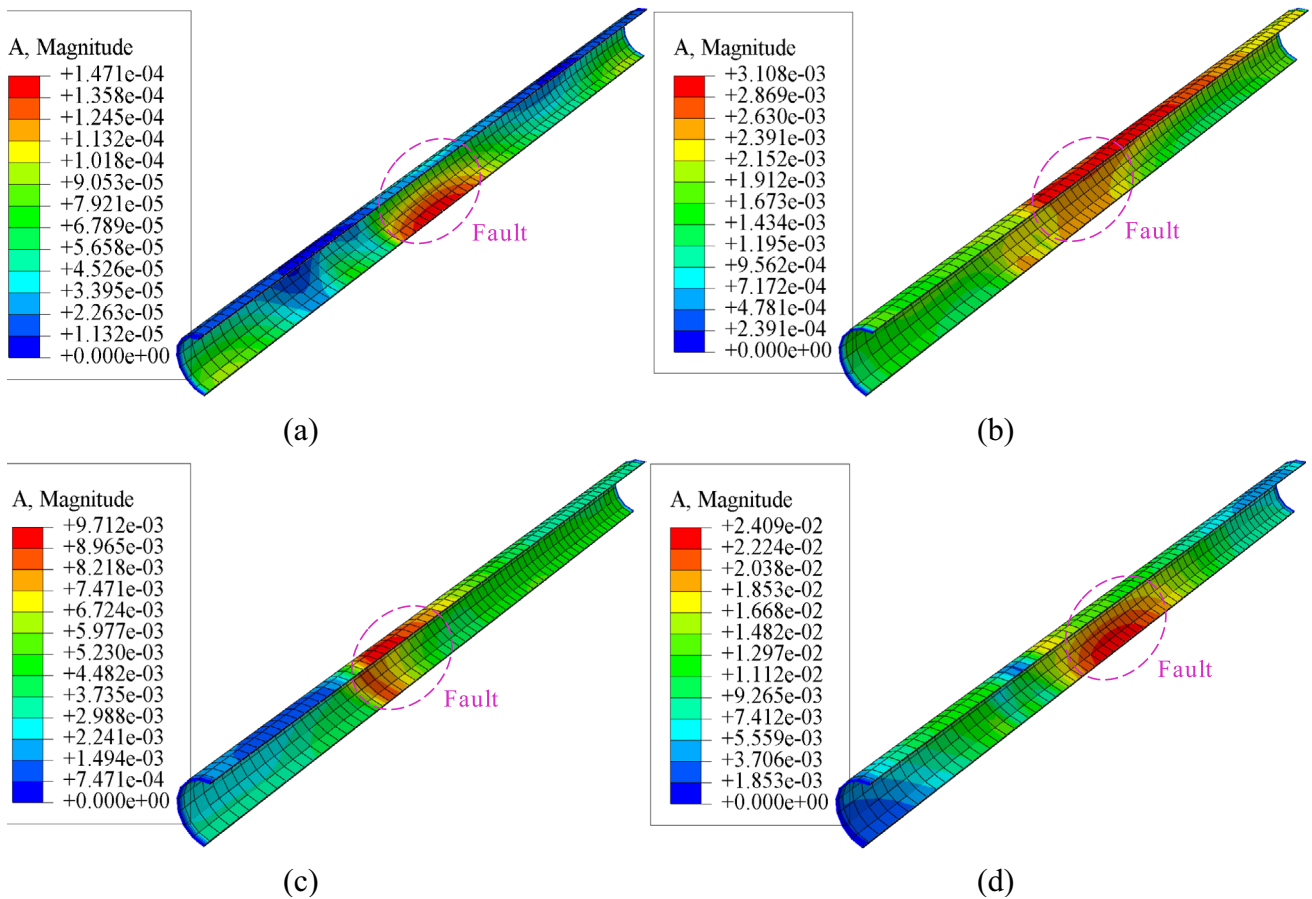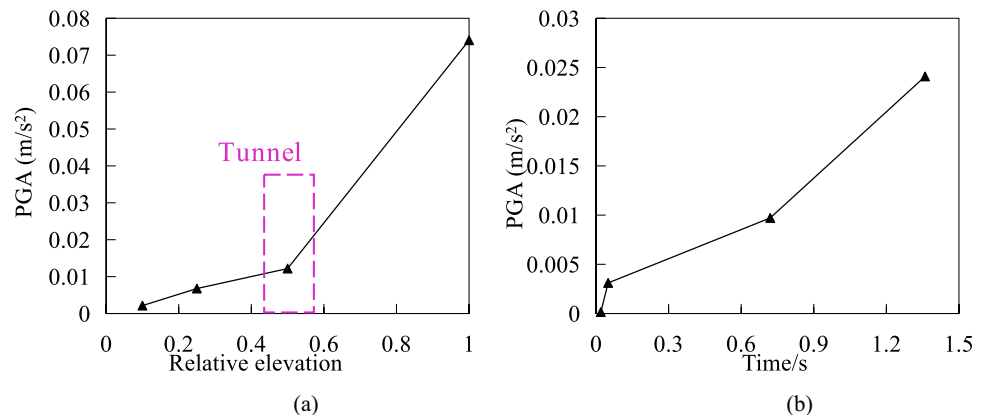

Fig. 8 Characteristics of seismic wave propagation in the tunnel lining structure: **a** t = 0.02 s; **b** t = 0.05 s; **c** t = 0.72 s; **d** t = 1.36 s (Unit: m/s.^{2})

Fig. 9 Change in PGA during the wave propagation process: **a** PGA with the relative elevation in the fault; **b** PGA with the wave propagation time

surrounding rock in fault has an obvious amplification effect. Figure 9b shows that the PGA of tunnel lining structures across fault segments increases with the duration of ground motion. It indicates that the dynamic amplification effect of tunnel structures across fault segments gradually increases with the duration of ground motion in a certain complete wave propagation process. Therefore, the dynamic amplification effect of the surrounding rock and lining structure in the crossing-fault tunnel area is the largest during ground motion, and earthquake damage is most likely to occur. It is the main reason why this study focuses on the seismic dynamic response of crossing-fault tunnels.

Dynamic amplification effect of the rock surrounding the tunnel

To further study the dynamic response characteristics of the tunnel surrounding rock, typical measuring points of the complete surrounding rock and fault surrounding rock are selected for analysis, as shown in Fig. 5b. The acceleration-time histories of some typical measuring points

are shown in Fig. 10. The variation rule of the PGA of the surrounding rock measurement points and the distance between faults is shown in Figs. 11 and 12. Figure 11a shows that with the fault as the axis of symmetry, the PGA of the surrounding rock measurement points (A7, A6, A4, A2) in the footwall area below the tunnel is larger than that of the measurement points (A17, A19, A21, A23) in the hanging wall area above the tunnel. This indicates that the dynamic response of the rock surrounding the footwall under the tunnel is greater than that of the hanging wall. Figure 11b shows that the PGA of the hanging wall rock (A20, A22, and A24) at the lower part of the tunnel is larger than that of the surrounding rock (A5, A3, and A1) at the upper part of the tunnel. This indicates that the dynamic amplification effect of the hanging wall area at the lower part of the tunnel is greater. The existence of the tunnel structure influences the dynamic amplification effect of the surrounding rock of the fault. The dynamic magnification effect of the footwall surrounding rock above the tunnel is large, while the dynamic magnification effect of the footwall surrounding rock below the
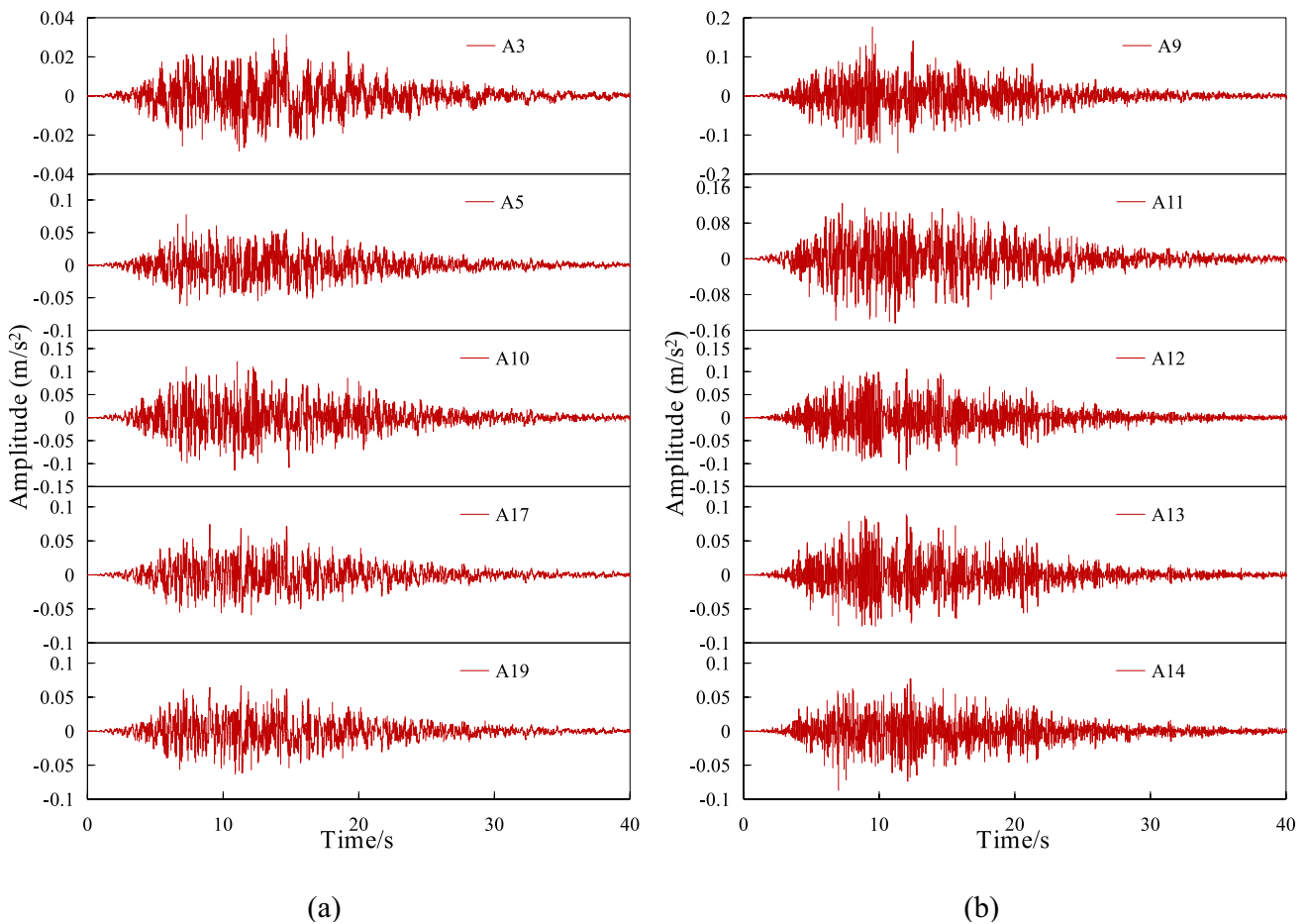

Fig. 10 Acceleration time histories of the surrounding rock above the tunnel: **a** above the tunnel; **b** in the fault (Unit: m/s.²)

Fig. 11 PGA comparison of the surrounding rocks of the upper and lower walls of the fault: **a** footwall below the tunnel and hanging wall above the tunnel; **b** footwall above the tunnel and hanging wall below the tunnel
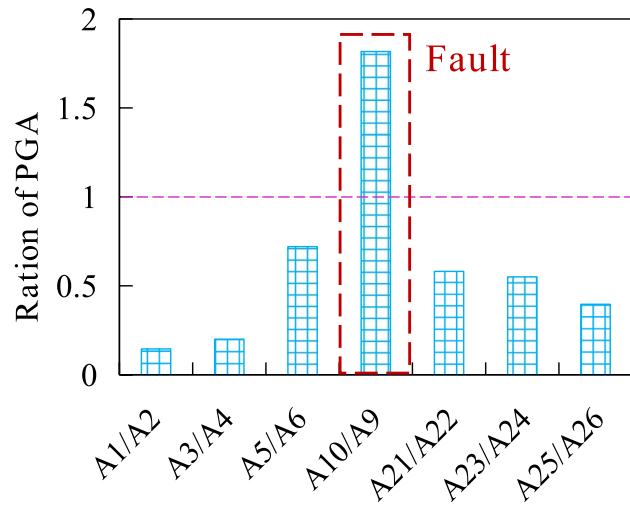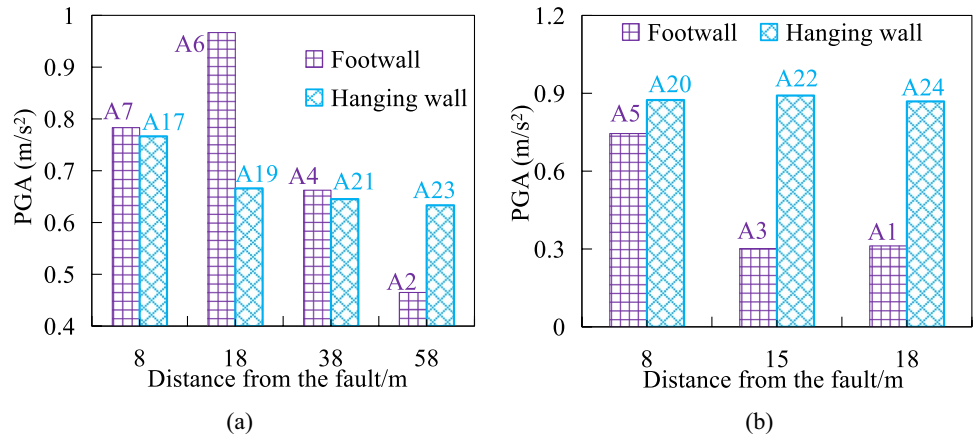

(a)

(b)

Fig. 12 Ratio of PGA above the tunnel to that below the tunnel

tunnel is small. Therefore, the tunnel has a small effect on the dynamic magnification effect of the intact surrounding rock area except for the fault.

In addition, the ratio of the PGA of the surrounding rocks above and below the tunnel is shown in Fig. 12. Figure 12 shows that except for measurement point A10/A9 (fault surrounding rock), the PGA ratio of the intact surrounding rock above the tunnel to below the tunnel is less than 1.0. While the A10/A9 ratio of the surrounding rock in the fault area is greater than 1.0. This indicates that the tunnel has a weakened effect on the dynamic amplification effect of the intact surrounding rock area but has an amplification effect on the dynamic response of the surrounding rock in the fault area. This is because the strength parameters of the surrounding rock in the fault fracture zone are small, and the integrity of the rock mass is poor. The integrity and strength of the surrounding rock in the fault area are enhanced by the tunnel structure, which magnifies the dynamic amplification effect of the surrounding rock. In contrast, the tunnel destroys the strength and integrity of the intact surrounding rock and weakens the dynamic response of the intact surrounding rock. In addition, by analysing the PGA variation characteristics of the tunnel lining structure, the dynamic response law of the tunnel structure is studied, as shown in Fig. 13. The PGA of the tunnel structure decreases gradually and tends to a certain stable value as the distance from

Fig. 13 PGA variation in the tunnel lining with distance from the fault: **a** foot wall of the fault; **b** hanging wall of the fault
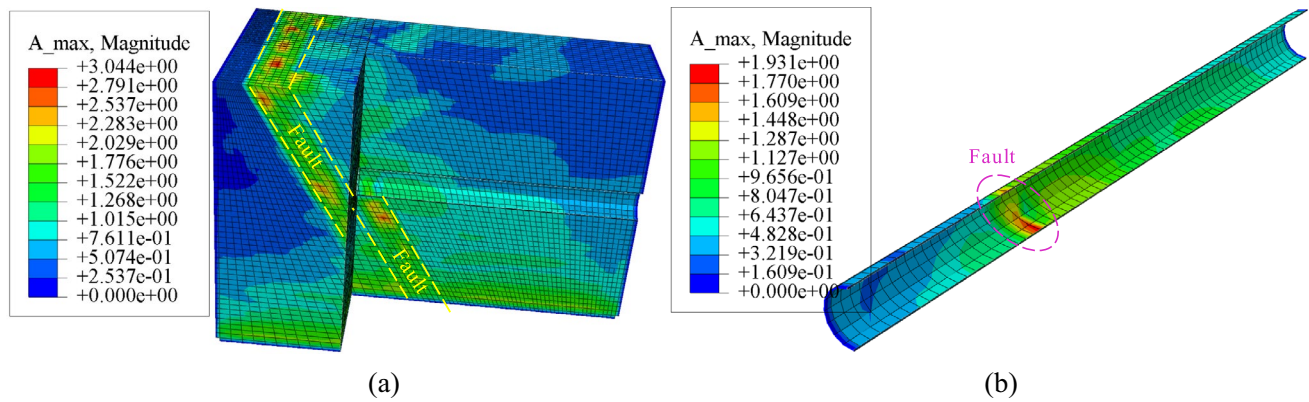

(a)

(b)
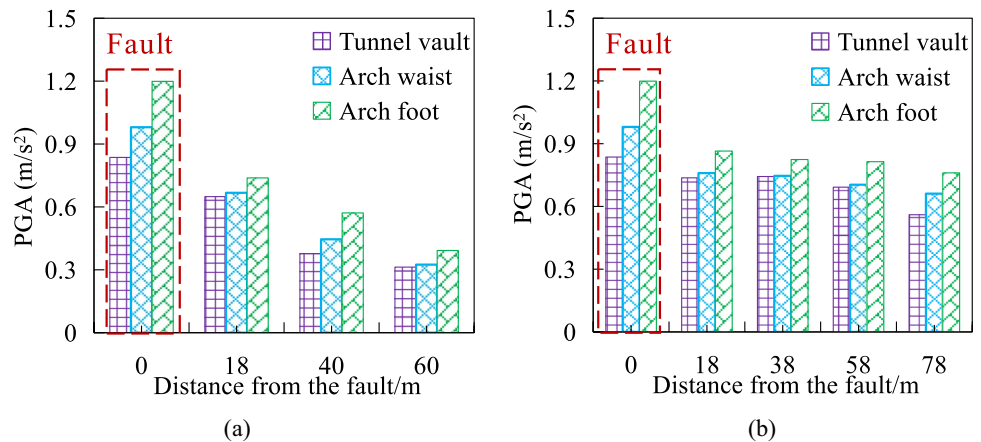
Fig. 14 Distribution characteristics of peak acceleration: **a** tunnel surrounding rock; **b** tunnel lining (Unit: m/s.^{2})

the fault increases. In the crossing-fault section, the PGA of the tunnel arch foot is larger than that of the arch waist. The PGA distribution of the surrounding rock and lining structure is shown in Fig. 14. The PGA maximum value of the surrounding rock is distributed in the fault area, and the PGA maximum value of the tunnel structure appears in the crossing-fault section. Therefore, compared with the intact surrounding rock tunnel structure, the PGA of the tunnel across the fault surrounding rock is the largest; and the crossing-fault surrounding rock and tunnel structure are most prone to instability failure under earthquakes.

Seismic response characteristics in the frequency

Modal analysis

The natural frequencies of the tunnel surrounding the rock and lining structure are related to the natural characteristics of the system. But it has nothing to do with the initial vibration conditions and vibration frequencies. When the system vibrates freely according to its natural frequency, the displacement of each particle in the system from its original equilibrium position satisfies a certain proportion relation. Mode refers to the vibration mode of the system when it vibrates according to a certain natural frequency, where the first mode is the main mode. Modal analysis is an important method of structural dynamic analysis and a basic type of dynamic frequency domain analysis, also known as natural frequency analysis. The finite element method is a common method in modal analysis to obtain the natural mode shape and natural frequency. Based on the principle of elasticity, the dynamic governing equation of modal analysis is as follows (Lee and Lee 2012; Reale et al. 2016):

$$[M]\{\ddot{U}\} + [C]\{\dot{U}\} + [K]\{U\} + \{F\} = 0 \tag{4}$$

where $[M]$, $[C]$, and $[K]$ are the mass matrix, damping matrix, and stiffness matrix, respectively. $\{F\}$ is the load function of the external force changing with time, and $\{\ddot{U}\}$ and $\{\hat{U}\}$ are the acceleration vector and velocity vector of the model, respectively. $\{U\}$ is the displacement vector of the model, which is used to describe the modal analysis of the mode shape. In the ideal case, the influence of external forces and damping effects are not considered in the modal analysis. The dynamic governing equation of modal analysis can be expressed as (Lee and Lee 2012; Reale et al. 2016):

$$[M]\{\ddot{U}\} + [K]\{U\} = 0 \tag{5}$$

Its characteristic equation is as follows:

$$\left([K] - \omega_i^2[M]\right)\{U\} = 0 \tag{6}$$

where ω_i is the ith natural circular frequency (i = 1,2,3…., n).

The natural frequency f_i obtained is as follows:

$$f_i = \frac{\omega_i}{2\pi} \tag{7}$$

The eigenvectors corresponding to the eigenvalues are $\{U\}_i$. $\{U\}_i$ represents the mode shape of vibration at natural frequency f_i. The first mode shape is the main mode shape, and the dynamic characteristics of the model are mainly controlled by the lower mode shapes. Only the first few modes are considered in the analysis.

The finite-element mode analysis is carried out on the numerical model of the surrounding rock of the crossing-fault tunnel. The modal shapes of the first three natural frequencies are shown in Fig. 15. The main mode shape under the condition of the first natural frequency vibration is shown in Fig. 15a. The first mode mainly causes a single deformation of the overall surrounding rock of the fault hanging and foot walls, including two torsional modes and
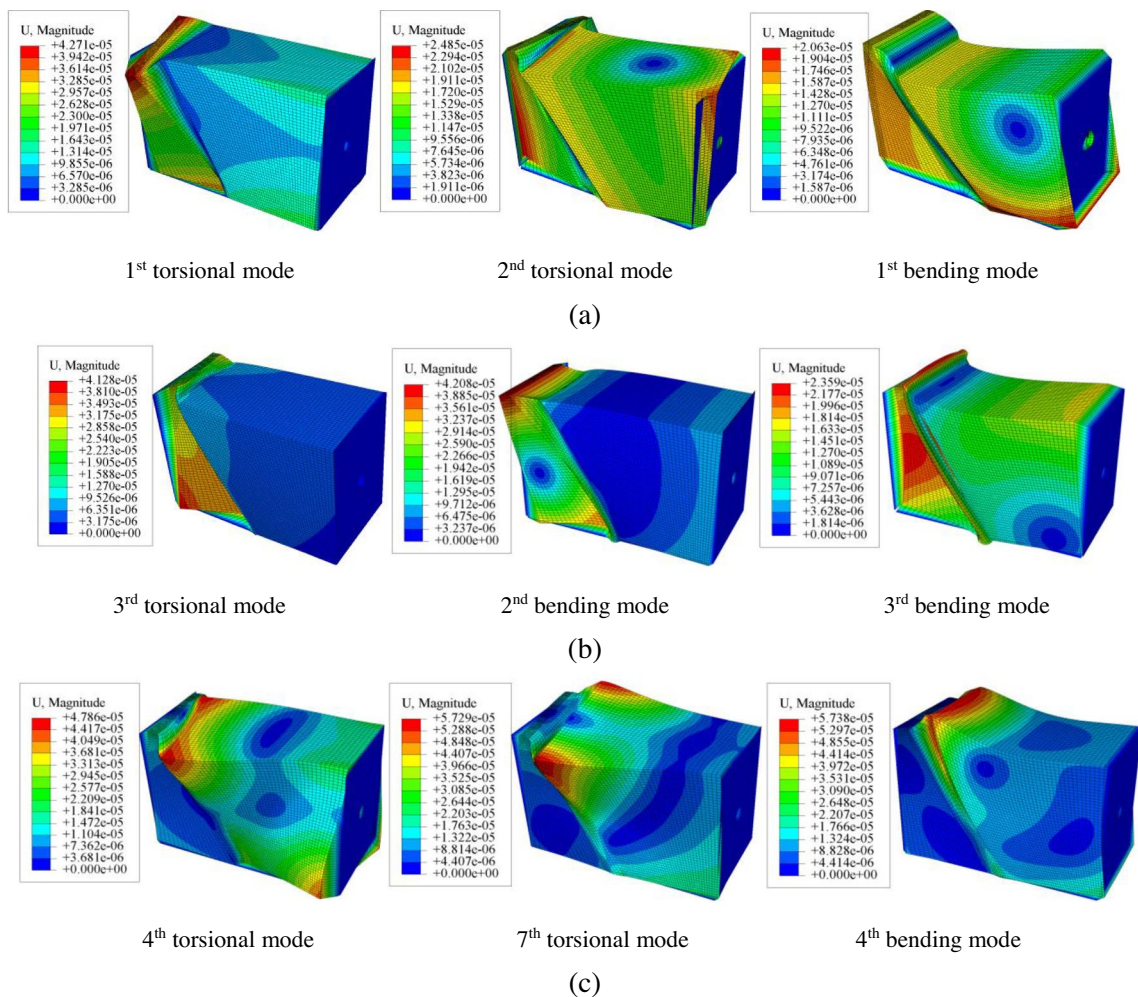
1st torsional mode   2nd torsional mode   1st bending mode

(a)

3rd torsional mode   2nd bending mode   3rd bending mode

(b)

4th torsional mode   7th torsional mode   4th bending mode

(c)

Fig. 15 Modal analysis of the model: **a** First mode; **b** second mode; **c** third mode

one bending mode. Figure 15b shows that the second-order natural frequency vibration mainly causes local single deformation of the footwall surrounding rock, including bending deformation and torsion deformation. Figure 15c shows that the third-order natural frequency vibration mainly causes local deformation in the surrounding rock of the fault hanging wall, including two local torsional deformations and one local bending deformation. The main mode corresponding to the first natural frequency is mainly characterized by the overall torsion and bending deformation characteristics of the surrounding rock of the fault hanging and foot walls. The modes corresponding to the higher (2nd and 3rd) natural frequencies are the local deformation characteristics of the surrounding rock of the fault. In other words, the first-order natural frequency mainly causes the overall deformation of the surrounding rock, while the higher-order natural frequency induces the local deformation of the surrounding

rock. Underground motions, the low-order and high-order natural frequencies of the rock surrounding the tunnel affect the deformation of the surrounding rock.

In addition, the tunnel lining structure is separately extracted from the surrounding rock, as shown in Fig. 16. Figure 16a shows that under the first natural frequency vibration, the vibration mode characteristics of the tunnel structure are the integral single deformation characteristics of the tunnel structure (torsion, bending or compression deformation). Figure 16b shows that the mode characteristics under the second-order natural frequency vibration are mainly affected by local single deformation of the crossing-fault tunnel structure. Figure 16c shows that under third-order natural frequency vibration, it is mainly manifested as a variety of combined local deformations of crossing-fault tunnel structures, which are specifically manifested as bending + compression deformation and torsional + bending deformation across fault segments. Therefore, the low (1st order) natural frequencies mainly
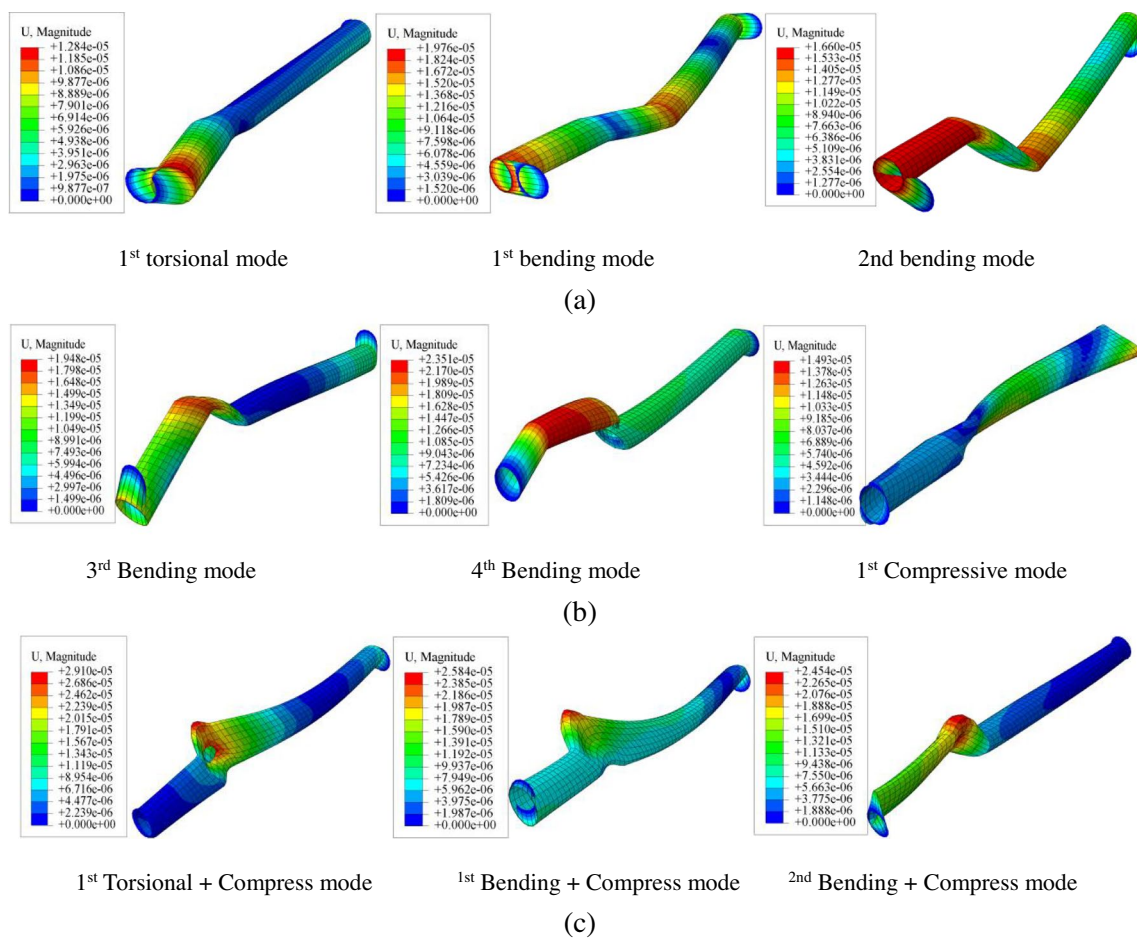
1st torsional mode　　　　　1st bending mode　　　　　2nd bending mode

(a)

3rd Bending mode　　　　　4th Bending mode　　　　　1st Compressive mode

(b)

1st Torsional + Compress mode　　　1st Bending + Compress mode　　　2nd Bending + Compress mode

(c)

Fig. 16 Modal analysis of the tunnel lining structure: **a** First mode; **b** second mode; **c** third mode

cause the overall deformation of the tunnel structure, while high (2nd and 3rd) natural frequencies mainly cause the deformation of the tunnel across the fault section.

Fourier spectrum analysis

The Fourier transform is the decomposition of seismic waves and other signals into a combination of harmonic signals, which is widely used in signal analysis and processing. The frequency-domain analysis mainly includes Fourier spectrum analysis and power spectrum analysis. Signal analysis based on the frequency domain can obtain the spectral response of rock and soil masses and the spectral characteristics of seismic waves. Fourier transform can be used to analyse the vibration response of the spectral characteristics of rock−soil masses and can also identify their seismic damage through the change in signal frequency components. The fast Fourier transform (FFT) has the advantage of good frequency location and can identify the different frequency components of the signal. The FFT can quickly identify the main components of the signal and has become a common

means of processing seismic wave signals. The essence of FFT is to decompose the seismic wave signal a(t) into a combination of multiple sine waves of different frequencies F(a). The different frequencies and their amplitudes that make up a sine wave can be identified based on the fast Fourier transform. However, the Fourier transform has some limitations when processing signals. The short-time Fourier transform adds a window to the signal along the time axis and assumes that the signal in the window is time-stable to realize the segmented Fourier transform of the whole signal. The Fourier spectrum has relatively serious energy leakage and low resolution, and it cannot be used for analysing nonstationary nonlinear signals. The mathematical expression of the FFT is shown as follows (Beylkin 1995):

$$F(a) = \int_{-\infty}^{+\infty} x(t)e^{-j2\pi at}dt \tag{8}$$

where a(t) is the acceleration history of the time domain and F(a) is the Fourier transform of the acceleration history a(t).

Fig. 17 Fourier spectrum of the surrounding rock above the tunnel: **a** below the tunnel; **b** above the tunnel

(a)

(b)

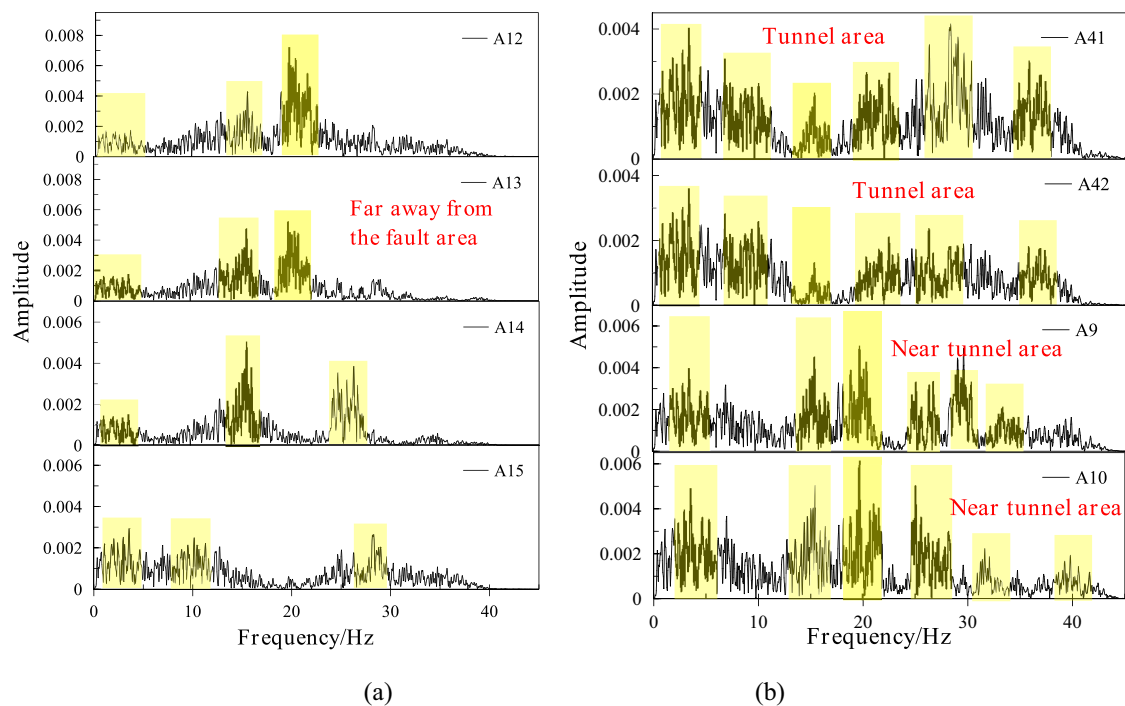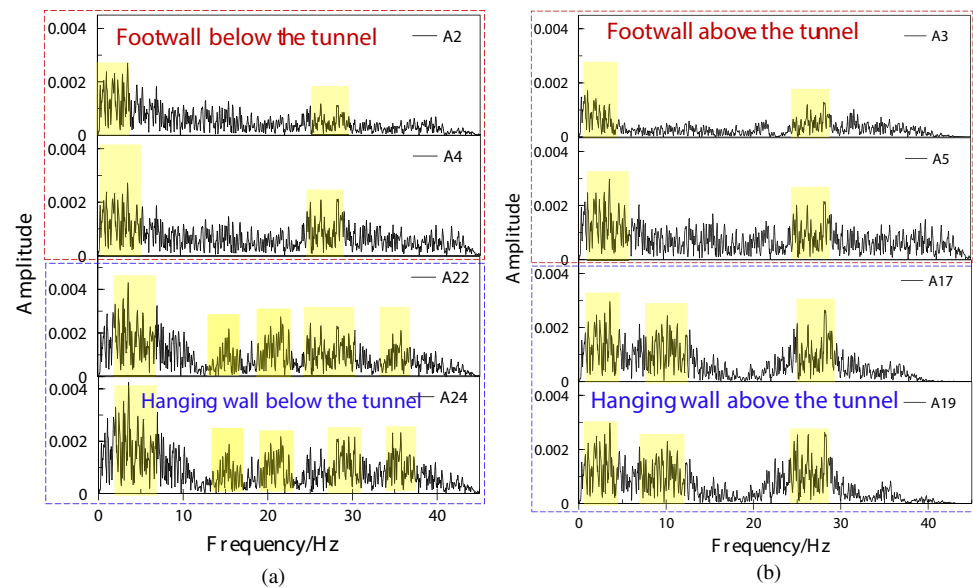(a)   (b)

Fig. 18 Fourier spectrum of the surrounding rock in the fault: **a** far away from the tunnel area; **b** near/in the tunnel area

To further analyse the tunnel surrounding rock by the Fourier spectrum, the Fourier spectrum of different measuring points is shown in Figs. 17 and 18. Figure 17a shows that the Fourier spectral characteristics of the measuring points in the surrounding rock above the tunnel are relatively simple, and the spectral characteristics of the measuring points on both sides of the fault are relatively similar overall. The fault only has a certain influence on the spectral amplitude at approximately 10 Hz. Figure 17b shows that the spectral

amplitudes of the footwall surrounding rock measurement points are relatively simple, while the spectral characteristics of the surrounding rock on the fault hanging wall are relatively complex. The number of natural frequencies increases from two to five, which affects the variation in the spectral amplitudes in some natural frequency segments. This shows that the fault has a great influence on the spectrum characteristics of the tunnel in the footwall area. The Fourier spectrum of eight typical measuring points in the fault

surrounding rock is analysed. By comparing the spectrum characteristics of the tunnel and the area near the tunnel, the influence of the tunnel on the dynamic response characteristics of the surrounding rock in the fault is studied. Figure 18a shows that the Fourier spectrum characteristics of the measuring points far from the fault are relatively simple, and the Fourier spectrum of the measuring points includes three excellent frequency segments. Figure 18b shows that in the fault surrounding rock, the Fourier spectrum characteristics of measuring points in the tunnel area and near the tunnel area are more complex than those in the surrounding rock far away from the tunnel area. It is obvious that the number of excellent frequency segments increases to six, and the amplification effect appears on more frequency components of the Fourier spectrum. The amplitude of the Fourier spectrum changes greatly in both high- and low-frequency bands. This shows that the tunnel has a great influence on the Fourier spectral characteristics of the fault surrounding rock, which enriches the frequency components of the spectral characteristics and increases the excellent frequency segment at the same time. This is because the interaction between the fault and tunnel makes the dynamic response characteristics of the surrounding rock more complex. In other words, from the perspective of Fourier spectrum analysis in the frequency domain, the tunnel makes the dynamic amplification effect of the crossing-fault surrounding rock greater. Therefore, its dynamic response is the most violent and prone to dynamic instability and failure.

To further analyse the influence of the tunnel on the Fourier spectrum characteristics of the intact surrounding rock and the crossing-fault surrounding rock, the Fourier spectrum of five typical sections I-I, II-II, IV-IV, V-V, and VIII-VIII (Fig. 4) was selected for analysis, as shown in Fig. 19. The spectrum ratio curves of the upper and lower measurement points of the tunnel with different sections are shown in Fig. 20. Figure 19 shows that the Fourier spectrum characteristics of the intact surrounding rock sections (I-I, II-II, V-V, VIII-VIII) above and below the tunnel are similar on the whole, and only the amplitude changes to a certain extent and the spectral peak above the tunnel decreases. Figure 20a shows that the spectral ratios of the upper and lower measurement points of the tunnel with intact surrounding rock sections are less than 1.0 on the whole, especially in the predominant frequency segment. In some non-excellent frequency segments, the spectral ratio is greater than 1.0. This shows that the tunnel has little influence on the spectral characteristics of the Fourier segment of the intact surrounding rock, and the tunnel has a weakening effect on its spectral amplitude. The tunnel reduces the transfer of seismic wave energy in the intact surrounding rock. Combined with the Fourier spectrum (Fig. 18b) and spectral ratio curve (Fig. 20b) of measuring points A9 and A10 (sections IV-IV) above and below the fault surrounding rock, the Fourier spectrum characteristics of the crossing-fault surrounding rock are similar, and the spectral ratio is larger than 1.0 overall. This shows that the tunnel has little influence on
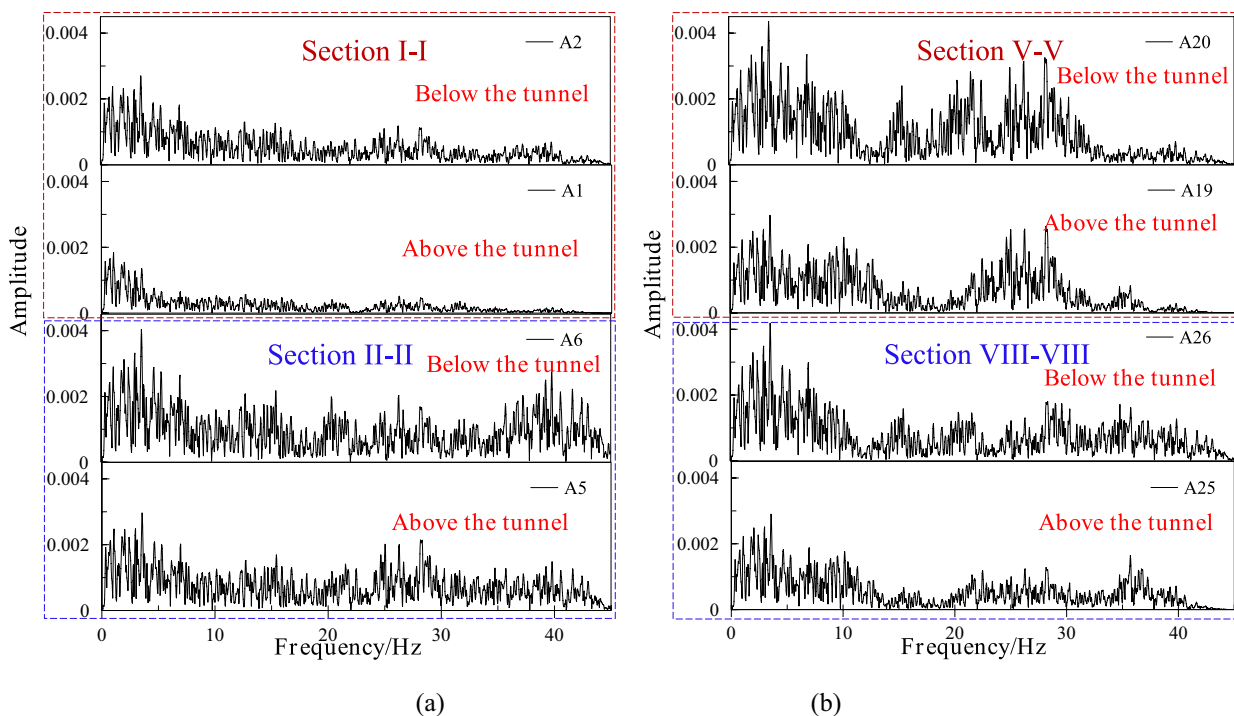

(a)　　　　　　　　　　　　　　　　(b)

Fig. 19 Fourier spectrum ratio of different sections in the numerical model: **a** footwall; **b** hanging wall
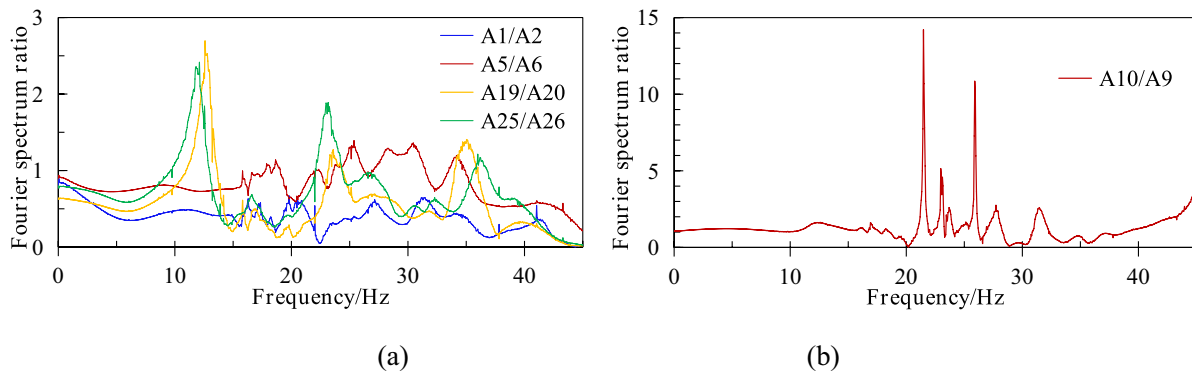
Fig. 20 Fourier spectrum ratio of different sections in the numerical model: **a** intact surrounding rock; **b** fault surrounding rock

the spectral characteristics in the crossing-fault section. But it has an amplification effect on the spectral peak. In addition, the peak Fourier spectral amplitude (PFSA) of different measuring points is selected to study the variation law of the surrounding rock with the distance from the fault, as shown in Fig. 21. The PFSA of the crossing-fault surrounding rock is the largest, which gradually decreases with the increasing distance from the fault and tends to a certain stable value. This indicates that the dynamic amplification effect of the crossing-fault segment is the largest, which is consistent with the results of the time domain and modal analysis.

Discussions

This work uses the finite-element method to study the seismic response characteristics of crossing-fault tunnels. From the time-domain perspective, the characteristics of wave propagation in the cross-fault tunnel under an earthquake are identified. The dynamic amplification effect of the crossing-fault tunnel and surrounding rock is explored, and the influence of the tunnel on the dynamic response of the surrounding rock is also analysed. Furthermore, modal analysis

and Fourier spectrum analysis are included in the analysis framework of the dynamic response frequency domain of the crossing-fault tunnel. Modal analysis intuitively illustrates the relationship between natural frequency and dynamic deformation of the cross-fault tunnel characteristics. Fourier spectrum analysis can be used to study the seismic response characteristics of rock surrounding a tunnel under earthquakes based on changes in spectral features. Fourier spectrum analysis and modal analysis results are mutually verified and supplemented, making the analysis results of the dynamic response in the frequency domain of the crossing-fault tunnel more comprehensive and reliable. In addition, the combination of time-domain and frequency-domain analysis reveals that the dynamic response of the cross-fault tunnel is quite different from the intact surrounding rock. Due to the refraction and reflection of seismic waves, in the surrounding rock across the fault, the local amplification is present. This also makes the deformation of the surrounding rock and lining structure across the fault section more obvious. This is also the reason why instability is more likely to occur across fault segments when it is subjected to seismic action. The shaking table model test results carried out by

Fig. 21 PFSA variation in the tunnel lining with distance from the fault: **a** footwall; **b** hanging wall
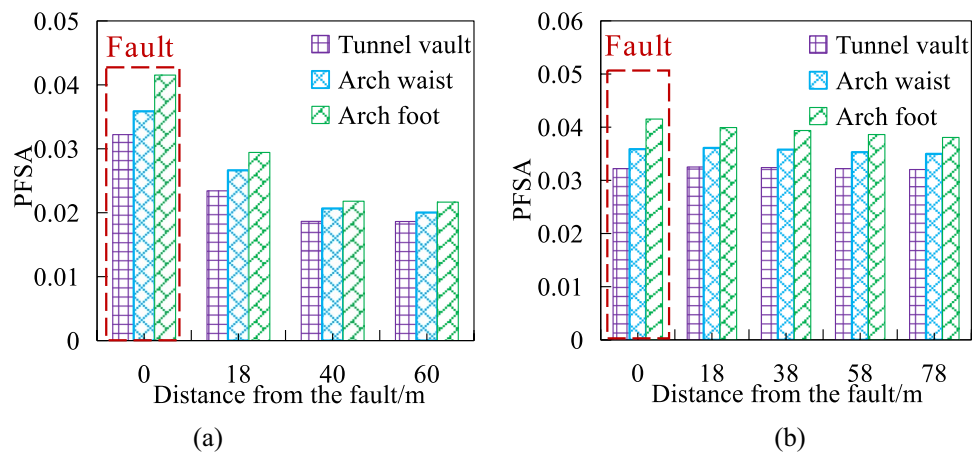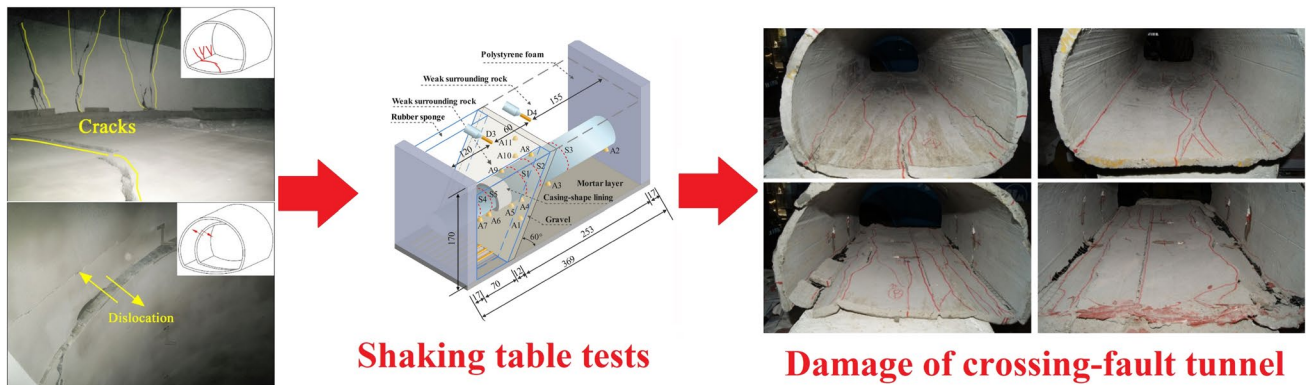
Fig. 22 Shaking table model test results (Xin et al. 2022)

Xin et al. (2022) verified the results of the numerical simulation (Fig. 22).

In general, time-domain analysis mainly studies the dynamic response of crossing-fault tunnels in mechanical deformation. In contrast, frequency-domain analysis mainly studies the dynamic response of cross-fault tunnels in natural characteristics. The analysis results of the time and frequency domains are mutually verified and supplemented, which improves the systematic and comprehensive understanding of the dynamic response of the crossing-fault tunnel. However, this work also has shortcomings. The surrounding rock of the crossing-fault tunnel is usually rich in fissure water. The dynamic response of the rock surrounding the crossing-fault tunnel is more complex under the coupling effect of earthquakes and fissure water. It is more critical to study the mechanism of hydrodynamic coupling disaster in crossing-fault tunnels surrounding rock, which will be researched in future work. In addition, the finite element method adopted in this work cannot be used to study the seismic damage evolution process in crossing-fault tunnels with strong earthquakes. In the future, the continuous-discontinuous medium coupled mechanical numerical method and shaking table model tests will be applied to study the damage of surrounding rock with water-bearing faults under earthquakes.

Conclusions

In this work, the finite-element numerical method is used to study the dynamic response characteristics of crossing-fault tunnels, and the main conclusions are shown as follows:

(1). A joint analysis method of time and frequency domains is proposed for the dynamic response of crossing-fault tunnel surrounding rock, and the analysis results of the time and frequency domains are mutually verified and complemented. By analysing the wave propagation and PGA variation, the dynamic response characteristics of the crossing-fault tunnel are analysed from the perspective of mechanics in the time domain. Combined with modal and Fourier spectrum analysis, the correlation mechanism of the wave's predominant frequency, the natural frequency of the surrounding rock, and its dynamic response characteristics are revealed. Modal analysis is more intuitive and concise, and the results were verified with the Fourier spectrum analysis method in spectral characteristics. Modal and Fourier spectrum analysis constitute a perfect frequency domain analysis framework for characterizing the dynamic response of surrounding rock in crossing-fault tunnels.

(2). The tunnel structure influences the characteristics of dynamic response in a crossing-fault tunnel, and the influences on the intact surrounding rock and crossing-fault section are different. The tunnel structure can influence the amplitude of the surrounding rock. However, it has little influence on the wave and Fourier spectrum characteristics of the surrounding rock. The dynamic amplification effect of the tunnel structure on the surrounding rock in the fault is obvious, and the dynamic amplification effect of the crossing-fault tunnel structure increases gradually with the duration of ground motion during wave propagation. The dynamic amplification effect of the intact surrounding rock is weakened by the tunnel, and the dynamic amplification effect of the intact surrounding rock above the tunnel is small.

(3). Faults have a controlling effect on the wave propagation characteristics in the rock surrounding the tunnel. During wave propagation, the fault is the main transmission channel of ground motion energy, which has the effect of amplifying wave transmission. During ground motions, the dynamic amplification effect

of the crossing-fault tunnel surrounding the rock and lining structure is the largest, and the earthquake damage is most likely to occur first. In the crossing-fault section, the dynamic amplification effect of the tunnel arch foot is larger than that of the arch waist, and that of the vault is the lowest.

(4). The dynamic deformation characteristics of the crossing-fault tunnel are clarified via modal analysis. The first natural frequency mainly causes the overall deformation of the surrounding rock, while the higher natural frequency induces the local deformation of the surrounding rock. The lower and higher natural frequencies of the surrounding rock have a joint effect on the deformation of the surrounding rock's underground motion. Low natural frequencies mainly cause the overall deformation of the tunnel structure, while high natural frequencies mainly cause the deformation of the tunnel in crossing-fault section.

Data availability Some or all data, models, or code that support the findings of this study are available from the corresponding author upon reasonable request.

References

Aygar EB, Gokceoglu C (2021) A special support design for a large-span tunnel crossing an active fault (T9 Tunnel, Ankara-Sivas High-Speed Railway Project, Turkey). Environ Earth Sci 80(1):37. https://doi.org/10.1007/s12665-020-09328-1

Bettess P, Zienkiewicz OC (1977) Diffraction and refraction of surface waves using finite and infinite elements. Int J Numer Meth Eng 11(8):1271–1290. https://doi.org/10.1002/nme.1620110808

Beylkin G (1995) On the fast Fourier transform of functions with singularities. Appl Comput Harmon Anal 2(4):363–381. https://doi.org/10.1006/acha.1995.1026

Cividini A, Gioda G, Petrini V (2010) Finite element evaluation of the effects of faulting on a shallow tunnel in alluvial soil. Acta Geotech 5(2):113–120. https://doi.org/10.1007/s11440-010-0116-1

Dou S, He L, Deng J, Wang NQ (2018) Application of modal analysis in acoustic-vibration detection of tunnel secondary liner void. J Railw Eng Soc 35(03):52–56. https://doi.org/10.3969/j.issn.1006-2106.2018.03.009

Fan L, Chen JL, Peng SQ, Qi BX, Zhou QW, Wang F (2020) Seismic response of tunnel under normal fault slips by shaking table test technique. J Central South University 27(4):1306–1319. https://doi.org/10.1007/s11771-020-4368-0

Geng Q, Zhang HJ, Liu XH, Wang XB (2019) Numerical study on the rock muck transfer process of TBM cutterhead with clump strategy based on discrete element method. Tunn Undergr Space Technol 91:103000. https://doi.org/10.1016/j.tust.2019.103000

Geng P, Zeng GX, Guo XY, He Y, Ding T, He C (2020) Seismic response of tunnel structures passing through fault zone under near-field pulsed earthquakes. China J Highw Trans 33(5):122–131

Goodman RE, Bray JW (1976) Toppling of rock slopes. Rock engineering for foundations & slopes, pp 201–234

Huang JQ, Zhao M, Du X (2017) Non-linear seismic responses of tunnels within normal fault ground under obliquely incident P waves. Tunn Undergr Space Technol 61:26–39. https://doi.org/10.1016/j.tust.2016.09.006

Kuhlemeyer RL, Lysmer J (1973) Finite element method accuracy for wave propagation problems. J Soil Mech Found Div 99(5):421–427. https://doi.org/10.1061/JSFEAQ.0001885

Kumar R, Kaur M (2014) Reflection and refraction of plane waves at the interface of an elastic solid and microstretch thermoelastic solid with micro temperatures. Arch Appl Mech 84(4):571–590. https://doi.org/10.1007/s00419-014-0818-1

Lee JH, Lee BS (2012) Modal analysis of carbon nanotubes and nano cones using FEM. Comput Mater Sci 51(1):30–42. https://doi.org/10.1016/j.commatsci.2011.06.041

Li JC, Ma GW (2009) Experimental study of stress wave propagation across a filled rock joint. Int J Rock Mech Min Sci 46(3):471–478. https://doi.org/10.1016/j.ijrmms.2008.11.006

Li SC, Wang ZC, Ping Y, Zhou Y, Zhang L (2014) Discrete element analysis of hydromechanical behaviour of a pilot underground crude oil storage facility in granite in China. Tunn Undergr Space Technol 40:75–84. https://doi.org/10.1016/j.tust.2013.09.010

Li CQ, Ding LY, Zhong BT (2019) Highway planning and design in the Qinghai-Tibet Plateau of China: A cost-safety balance perspective. Engineering 5(2):337–349. https://doi.org/10.1016/j.eng.2018.12.008

Liang JW, Xu AQ, Ba ZN, Chen RD, Zhang W, Liu MG (2021) Shaking table test and numerical simulation on ultra large diameter shield tunnel passing through soft-hard stratum. Soil Dyn Earthq Eng 147:106790. https://doi.org/10.1016/j.soildyn.2021.106790

Liu EL, Huang RQ, He SM (2012) Effects of frequency on the dynamic properties of intact rock samples subjected to cyclic loading under confining pressure conditions. Rock Mech Rock Eng 45(1):89–102. https://doi.org/10.1007/s00603-011-0185-y

Liu GQ, Zhang YH, Ren JQ, Xiao M (2021) Seismic response analysis of tunnel through fault considering dynamic interaction between rock mass and fault. Energies 14(20):19. https://doi.org/10.3390/en14206700

Long X, Ma Y, Miao Y, Ruan B (2023) An innovative shape memory alloy flexible circumferential joint for tunnel seismic mitigation. Tunn Undergr Space Technol 131:104783. https://doi.org/10.1016/j.tust.2022.104783

Lu C, Cai C (2019) Challenges and countermeasures for construction safety during the sichuan-tibet railway project. Engineering 5(5):833–838. https://doi.org/10.1016/j.eng.2019.06.007

Ma YLN, Sheng Q, Zhang GM, Cui Z (2019) A 3D discrete-continuum coupling approach for investigating the deformation and failure mechanism of tunnels across an active fault: A case study of Xianglushan Tunnel. Appl Sci 9(11):17. https://doi.org/10.3390/app9112318

Madsen PA (1983) Wave reflection from a vertical permeable wave absorber. Coast Eng 7(4):381–396. https://doi.org/10.1016/0378-3839(83)90005-4

Mahtab MA (1970) Three dimensional finite element analysis of jointed rock slopes. Int Soc Rock Mech Proc

Ngo D, Scordelis AC (1967) Finite element analysis of reinforced concrete beam. J Proc 64(3):152–163. https://doi.org/10.14359/7551

Pai LF, Wu HG (2021) Multi-attribute seismic data spectrum analysis of tunnel orthogonal underpass landslide shaking table test. Soil Dyn Earthq Eng 150:106889. https://doi.org/10.1016/j.soildyn.2021.106889

Reale C, Gavin K, Prendergast LJ, Xue JF (2016) Multi-modal reliability analysis of slope stability. Trans Res Procedia 14:2468–2476. https://doi.org/10.1016/j.trpro.2016.05.304

Shen YS, Wang ZZ, Yu J, Zhang X, Gao B (2020) Shaking table test on flexible joints of mountain tunnels passing through normal fault. Tunn Undergr Space Technol 98:103299. https://doi.org/10.1016/j.tust.2020.103299

Shi WP, Zhang JW, Song DQ, Liu XL, Wang EZ, Zhao JJ (2024) Dynamic response characteristics and instability mechanism of high-steep bedding rock slope at the tunnel portal in high-intensity seismic region. Rock Mech Rock Eng 57(2):827–849. https://doi.org/10.1007/s00603-023-03629-0

Song DQ, Che AL, Zhu RJ, Ge XR (2019) Natural frequency characteristics of rock masses containing a complex geological structure and their effects on the dynamic stability of slopes. Rock Mech Rock Eng 52(11):4457–4473. https://doi.org/10.1007/s00603-019-01885-7

Song D, Liu X, Chen Z, Chen J, Cai J (2020a) Influence of tunnel excavation on the stability of a bedded rock slope: A case study on the Mountainous area in Southern Anhui. China KSCE J Civil Eng 25(1):114–123. https://doi.org/10.1007/s12205-020-0831-6

Song DQ, Chen Z, Ke YT, Nie W (2020b) Seismic response analysis of a bedding rock slope based on the time-frequency joint analysis method: a case study from the middle reach of the Jinsha River. China Engineering Geology 274:105731. https://doi.org/10.1016/j.enggeo.2020.105731

Song DQ, Liu XL, Huang J, Wang EZ, Zhang JM (2021) Characteristics of wave propagation through rock mass slopes with weak structural planes and their impacts on the seismic response characteristics of slopes: a case study in the middle reaches of Jinsha River. Bull Eng Geol Environ 80(2):1317–1334. https://doi.org/10.1007/s10064-020-02008-1

Song D, Zhang S, Liu C, Nie W (2024) Cumulative damage evolution of jointed slopes subject to continuous earthquakes: influence of joint type on dynamic amplification effect and failure mode of slopes. Comput Geotech 166:106016. https://doi.org/10.1016/j.compgeo.2023.106016

Sun TC, Gao B, Huang M, Wang ZZ (2009) Applications of time-frequency analysis on earthquake wave in the dynamic response analysis of tunnel. J Beijing Univ Technol 35(11):1491–1498. https://doi.org/10.11936/bjutxb2009111491

Sun BB, Deng MJ, Zhang SR, Cui W, Wang C, Yu LC, Cao KL (2020) Inelastic dynamic analysis and damage assessment of a hydraulic arched tunnel under near-fault SV waves with arbitrary incoming angles. Tunn Undergr Space Technol 104:103523. https://doi.org/10.1016/j.tust.2020.103523

Wei X, Gao WX, Wang LT, Cao XL (2019) Analysis and application of metro tunnel blasting vibration signal based on EEMD. Tunnel Constr 39(08):1293–1300. https://doi.org/10.3973/j.issn.2096-4498.2019.08.010

Xin C, Wang Z, Hajirasouliha I, Yang F, Li W, Chen T, Gao B (2022) Seismic response mechanisms of casing-shape composite tunnel lining: Theoretical analysis and shaking table test verification. Soil Dyn Earthq Eng 162:107440. https://doi.org/10.1016/j.soildyn.2022.107440

Xu XJ, Zhang PL, Guo X, Liu B, Chen L, Zhang QS, Nie LC, Zhang Y (2021) A case study of seismic forward prospecting based on the tunnel seismic while drilling and active seismic methods. Bull Eng Geol Env 80(5):3553–3567. https://doi.org/10.1007/s10064-020-02088-z

Yan GM, Gao B, Shen YS, Zheng Q, Fan KX, Huang HF (2020) Shaking table test on seismic performances of newly designed joints for mountain tunnels crossing faults. Adv Struct Eng 23(2):248–262. https://doi.org/10.1177/1369433219868932

Yu H, Chen J, Bobet A, Yuan Y (2016) Damage observation and assessment of the Longxi tunnel during the Wenchuan earthquake. Tunn Undergr Space Technol 54:102–116. https://doi.org/10.1016/j.tust.2016.02.008